

## Single-Crystal CdSe Nanosaws

Christopher Ma, Yong Ding, Daniel Moore, Xudong Wang, and Zhong Lin Wang\*

School of Materials Science and Engineering, Georgia Institute of Technology, Atlanta, Georgia 30332-0245

Received November 12, 2003; E-mail: zhong.wang@mse.gatech.edu

Wurtzite-structured cadmium selenide (CdSe) is an important II-VI semiconducting compound for optoelectronics.<sup>1</sup> CdSe quantum dots are the most extensively studied quantum nanostructure due to their size-tunable properties, and they have been used as a model system for investigating a wide range of nanoscale electronic, optical, optoelectronic, and chemical processes.<sup>2</sup> CdSe was also the first example of self-assembled semiconductor nanocrystal superlattices.<sup>3</sup> With a direct band gap of 1.8 eV, CdSe quantum dots have been used for laser diodes,<sup>4</sup> nanosensing,<sup>5</sup> and biomedical imaging.<sup>6</sup>

Although CdSe quantum dots have been the dominant material for studying the quantum confined effect, there are only a few reports on the synthesis of quasi-one-dimensional CdSe nanostructures. Shape-controlled synthesis of CdSe nanorods<sup>7,8</sup> and template-assisted synthesis of CdSe nanowires<sup>9</sup> and nanotubes<sup>10</sup> have been demonstrated through electrochemical and chemical approaches. Two-dimensional arrays of CdSe pillars have been fabricated using e-beam lithography.<sup>11</sup> These nanowire and nanotubes are composed of nanosize grains, and they are polycrystalline in nature; thus, the grain boundary scattering could greatly affect the optoelectronic performance. In this paper, we report, for the first time, a single-crystal nanoribbon structure of wurtzite CdSe, which has “saw”-shaped teeth on one side. The asymmetric growth behavior of the ribbon is likely induced by the polarization of the *c*-plane.

The CdSe nanobelts were synthesized through a thermal evaporation process in a horizontal tube furnace. Commercial-grade CdSe powder (Alfa Aesar, 99.995% purity, metal basis) was placed in the center of a single zone tube furnace (Thermolyne 79300) and evacuated for several hours to purge oxygen in the chamber. After the evacuation process was complete, the temperature of the system was elevated to 750 °C at a rate of 20 °C/min and the pressure was maintained at 300 mbar. Nitrogen was sent through the system at a rate of 50 sccm to act as a carrier gas to transport the sublimated vapor to cooler regions within the tube furnace for deposition. The system was held at these conditions for a period of 60 min. Single-crystal silicon substrates, dispersed with gold particles of typical sizes 3–5 nm, which acted as catalyst, were used for growing the nanostructure. The substrates were placed downstream to collect the deposited CdSe nanostructures.

The most dominant morphology found in the as-grown sample is the “saw”-shaped nanoribbon (Figure 1a), with one side flat and the other side with sharp teeth (Figure 1b, c). Nanobelts of CdSe are also found, but they are not the dominant component (Figure 1d).

Transmission electron microscopy shows that the nanosaw is a single-crystal, dislocation-free, and dominated by  $\pm(2-1-10)$  facets. The bending of the saw ribbon produces the bending contour as observed in the TEM image (Figure 2a). The saw teeth can be parallel cantilevers and triangular teeth. The front-end of the nanosaw ribbon clearly shows an Au particle, as indicated by an arrowhead, but the tips of the saw teeth show no catalyst particles. The structure of the saw can be separated into two segments. In

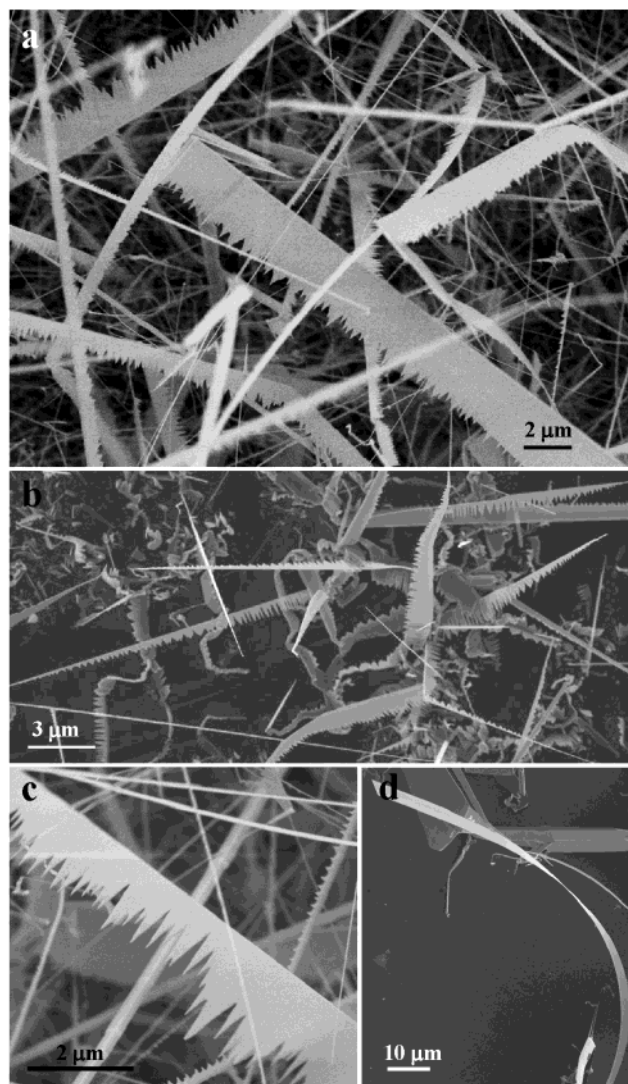
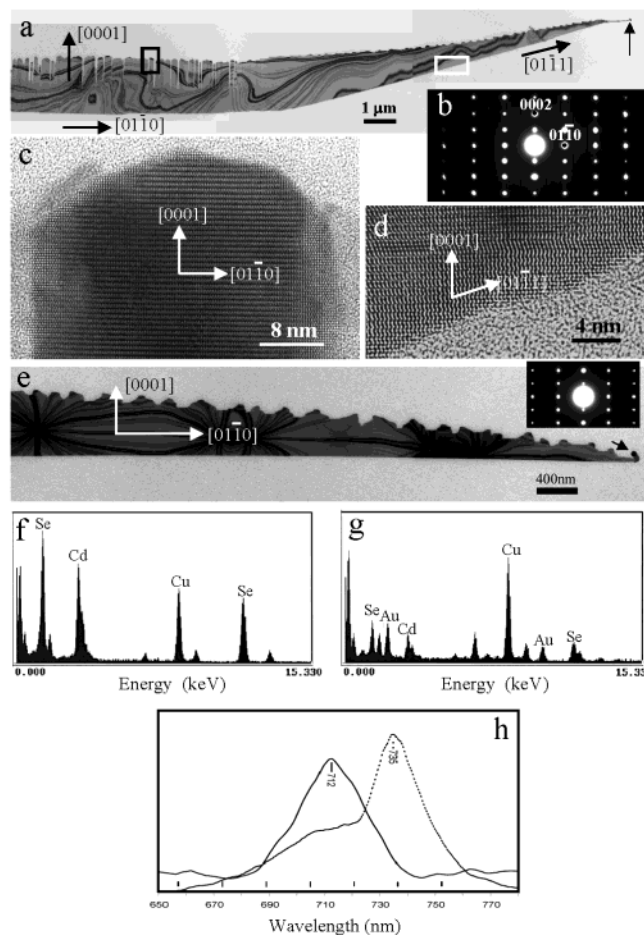


Figure 1. Scanning electron microscopy images of CdSe (a, b, c) nanosaws and (d) nanobelts.

the left-hand side of Figure 2a, where the parallel cantilever arrays along [0001] are formed, the saw ribbon extends along [0 1 -1 0]. High-resolution transmission electron microscopy (TEM) image shows that the end of the cantilever is atomically rough, clearly representing the growth front, while the side surfaces are atomically flat (Figure 2c). In the right-hand side of Figure 2a, where the triangular teeth are present, the saw ribbon is along [0 -1 -1 1] (Figure 2d).

The nanosaw is formed by a two-step growth process: the first step is a fast growth along [0 1 -1 0] or [0 1 -1 1] as guided by a gold catalyst based on the vapor–liquid–solid (VLS) growth process (see the SEM image in Figure 1b), forming a ribbon



**Figure 2.** (a) TEM image of a CdSe nanosaw and (b) the corresponding electron diffraction pattern, showing the ribbon direction is  $[0\ 1\ -1\ 0]$  and switches to  $[0\ 1\ -1\ -1]$ , while the teeth direction is  $[0001]$ . (c, d) High-resolution TEM images recorded from the areas indicated by black and white boxes in (a), respectively. The nanosaw has a high crystallinity and is free from dislocations, although stacking fault parallel to  $(0001)$  can be found occasionally. (e) TEM image of a CdSe nanosaw and the corresponding electron diffraction pattern. (f, g) Energy-dispersive X-ray spectra recorded from a nanosaw and the catalyst particle at the tip, where the Cu and carbon signals come from the TEM grid. The sample is dominated by Cd and Se, and the catalyst particle is dominated by Au. (g) UV photoluminescence measured from the CdSe powder (dotted line) and from CdSe nanosaw, which were measured under identical experimental conditions.

structure with the top and bottom surfaces being  $\pm(2\ -1\ -1\ 0)$  facets and the side surfaces being  $\pm(0001)$ ; the second step is a subsequent growth of the teeth along  $[0001]$ , which can be understood from the structure characteristic of the wurtzite family (Figure 2e). Energy-dispersive X-ray analysis shows that the sample is CdSe (Figure 2f) and the catalyst particle at the tip of the saw is mainly gold (Figure 2g).<sup>12</sup>

Structurally, the wurtzite-structured CdSe is described schematically as a number of alternating planes composed of four-fold coordinated  $\text{Cd}^{2+}$  and  $\text{Se}^{2-}$ , stacked alternatively along the  $c$ -axis. The  $c$ -plane terminates either with Cd or with Se, resulting in the formation of positively charged  $(0001)\text{-Cd}$  and negatively charged  $(0\ 0\ 0\ -1)\text{-Se}$  polar surfaces. The adsorption probability of the CdSe vapor onto the  $(0001)\text{-Cd}$ - and  $(0\ 0\ 0\ -1)\text{-Se}$ -terminated polar surfaces could be very different. As for ZnO, a typical wurtzite structure, it is known that the alcohols adsorbed dissociatively on

the  $(0001)\text{-Zn}$ -terminated surface to form alkoxide intermediates which decomposed to form net dehydration and/or net dehydrogenation products; in contrast, the  $(0\ 0\ 0\ -1)\text{-O}$  surface was found to be unreactive toward these alcohols; only molecular adsorption occurred on this surface.<sup>13</sup> For the decomposition reactions of methanol, formaldehyde, and formic acid,<sup>14</sup> the  $(0\ 0\ 0\ -1)\text{-O}$  polar face exhibited no reactivity, while the  $(0001)\text{-Zn}$  surface is active in oxidizing  $\text{HCOOH}$  and  $\text{CH}_2\text{O}$  into  $\text{CO}_2$ . Recent study shows that the  $(0001)\text{-Zn}$ -terminated surface is chemically active and it can be the self-catalyst for growing “comblike” structures.<sup>12</sup> Polar surfaces can also induce the formation of helicals of ZnO nanobelts.<sup>15</sup> Therefore, the formation of the one-sided saw teeth structure for CdSe reported here is suggested to be a result of the chemically active  $(0001)\text{-Cd}$  surface.

The optical property of the CdSe nanostructure was characterized by a UV photoluminescence (PL) system using a  $\text{N}_2$  pulse laser with an excitation wavelength of 337 nm. As compared to the PL spectrum acquired from the source CdSe powders, whose luminescence peak is located at 735 nm, the CdSe nanosaws show a peak at 712 nm (Figure 2h), shifted toward blue for 23 nm possibly because of the small thickness of the CdSe nanosaws.

In conclusion, single-crystal nanosaws and nanobelts of CdSe have been synthesized for the first time. The formation of the saw structure is likely induced by the surface polarization. The formation of the saw ribbon follows a VLS growth, while the saw teeth are the result of self-catalyzed growth possibly from the Cd-terminated  $(0001)$  surface. The photoluminescence spectrum of the nanosaws shows a blue shift of 23 nm. The nanosaw structure presented here could be a model system for investigating CdSe-based optoelectronic processes in quasi-one-dimensional nanostructures.

**Acknowledgment.** This research was supported by the NSF.

**Supporting Information Available:** Figure showing the structure model and the polar surfaces of the CdSe wurtzite structure (PDF). This material is available free of charge via the Internet at <http://pubs.acs.org>.

## References

- (1) (a) Hodes, G.; Albu-Yaron, A.; Decker, F.; Motisuke, P. *Phys. Rev. B* **1987**, *36*, 4215. (b) Ichimura, M.; Sato, N.; Nakamura, A.; Takeuchi, K.; Arai, E. *Phys. Status Solidi* **2002**, *193*, 132.
- (2) (a) Tolbert, S. H.; Alivisatos, A. P. *Science* **1994**, *265*, 373. (b) Bawendi, M. G.; Kortan, A. R.; Steigerwald, M. L.; Brus, L. E. *J. Chem. Phys.* **1989**, *91*, 7282.
- (3) Murray, C. B.; Kagan, C. R.; Bawendi, M. G. *Science* **1995**, *270*, 1335.
- (4) Colvin, V. L.; Schlamp, M. C.; Alivisatos, A. P. *Nature* **1994**, *370*, 354.
- (5) Tran, P. T.; Goldman, E. R.; Anderson, G. P.; Mauro, J. M.; Mattoussi, H. *Phys. Status Solidi* **2002**, *229*, 427.
- (6) (a) Chan, W. C.; Nie, S. M. *Science* **1998**, *281*, 2016. (b) Bruchez, M.; Moronne, M.; Gin, P.; Weiss, S.; Alivisatos, A. P. *Science* **1998**, *281*, 2013.
- (7) Peng, X. G.; Manna, L.; Yang, W. D.; Wickham, J.; Scher, E.; Kadavanich, A.; Alivisatos, A. P. *Nature* **2000**, *404*, 59.
- (8) Hu, J. T.; Li, L. S.; Yang, W. D.; Manna, L.; Wang, L. W.; Alivisatos, A. P. *Science* **2001**, *292*, 2060.
- (9) (a) Peng, X. S.; Zhang, J.; Wang, X. F.; Wang, Y. W.; Zhao, L. X.; Meng, G. W.; Zhang, L. D. *Chem. Phys. Lett.* **2001**, *343*, 470. (b) Xu, D. S.; Shi, X. S.; Guo, G. L.; Gui, L. L.; Tang, Y. Q. *J. Phys. Chem B* **2000**, *104*, 5061.
- (10) Jiang, X. C.; Mayers, B.; Herricks, T.; Xia, Y. N. *Adv. Mater.* **2003**, *15*, 1740.
- (11) Wu, Y. W.; Wu, C. S.; Chen, C. C.; Chen, C. D. *Adv. Mater.* **2003**, *15*, 49.
- (12) Wang, Z. L.; Kong, X. Y.; Zuo, J. M. *Phys. Rev. Lett.* **2003**, *91*, 185502.
- (13) Vohs, J. M.; Barteau, M. A. *Surf. Sci.* **1989**, *221*, 590.
- (14) Vohs, J. M.; Barteau, M. A. *Surf. Sci.* **1986**, *176*, 91.
- (15) Kong, X. Y.; Wang, Z. L. *Nano Lett.* **2003**, *3*, 1625.

JA0395644